

Electroreflectance measurements of electric fields in ordered GaInP₂

J. D. Perkins, Y. Zhang, J. F. Geisz, W. E. McMahon, J. M. Olson, and A. Mascarenhas

Citation: *Journal of Applied Physics* **84**, 4502 (1998); doi: 10.1063/1.368675

View online: <https://doi.org/10.1063/1.368675>

View Table of Contents: <http://aip.scitation.org/toc/jap/84/8>

Published by the *American Institute of Physics*

AIP | Journal of
Applied Physics

SPECIAL TOPICS



Electroreflectance measurements of electric fields in ordered GaInP₂

J. D. Perkins,^{a)} Y. Zhang, J. F. Geisz, W. E. McMahon, J. M. Olson, and A. Mascarenhas
National Renewable Energy Laboratory, Golden, Colorado 80401

(Received 8 May 1998; accepted for publication 10 June 1998)

Ordered Ga_{0.52}In_{0.48}P alloys (GaInP₂ for simplicity) grown on miscut [001] GaAs resemble monolayer superlattices with alternating Ga- and In-rich layers along either the $[\bar{1}11]$ or $[1\bar{1}1]$ directions. Recent calculations suggest that, in fully ordered GaInP₂, an intrinsic ordering-induced electric field of order 1600 kV/cm should exist. In partially ordered samples, as can actually be grown, the expected field is reduced to 400 kV/cm. For such a strong internal electric field, clear Franz-Keldysh Oscillations (FKOs) would be expected in an electroreflectance measurement. We report electroreflectance measurements of ordered GaInP₂ layers measured at $T=100$ K. For all samples measured, no FKOs are observed in the absence of an additional external dc bias voltage. At the lowest bias voltages for which FKOs are seen, the internal electric field in the GaInP₂ layer, determined from the FKOs, is ~ 60 kV/cm along the [001] direction corresponding to ~ 100 kV/cm along the ordering direction. Hence, we conclude that, at least in the organometallic vapor phase epitaxy grown samples studied here, any net macroscopic internal electric field in the GaInP₂ layer is less than ~ 100 kV/cm along the ordering direction. © 1998 American Institute of Physics. [S0021-8979(98)02418-9]

I. INTRODUCTION

Ga_{0.52}In_{0.48}P alloys (GaInP₂ for simplicity) grown by organometallic vapor phase epitaxy (OMVPE) on [001] GaAs substrates can exhibit a spontaneous CuPt-type ordering of various degrees along the $[\bar{1}11]$ or $[1\bar{1}1]$ directions, depending upon the growth conditions and substrate misorientation.¹⁻⁵ These structures resemble monolayer superlattices of Ga_{(1+ η)/2}In_{(1- η)/2}P/Ga_{(1- η)/2}In_{(1+ η)/2}P along the ordering direction. The ordering parameter, η , is zero for a random alloy and one for a perfectly ordered GaP and InP monolayer superlattice. An ordering parameter of $\eta \approx 0.5$ is readily achievable with careful control of the growth parameters.^{3,4,6} Such ordering both lowers the band-gap energy and splits the quadruply degenerate valence band states. These ordering-induced electronic structure changes have been well established by photoluminescence (PL),^{2,6} photoluminescence excitation,^{7,8} and polarized piezomodulation⁵ spectroscopies as well as more recent exciton absorption bleaching measurements.⁹ First-principles and perturbation based electronic structure calculations agree well with these experiments.¹⁰⁻¹⁸

However, recent first-principles calculations by Froyen *et al.*¹⁹ suggest that, in addition, for perfectly ordered undoped GaInP₂, an intrinsic electric field should exist along the ordering direction. For clarity of discussion, we take the ordering direction to lie along $[\bar{1}11]$. In one view, the predicted field is essentially piezoelectric in origin. In general, compound semiconductors with zinc-blende structure are piezoelectric along the $\langle 111 \rangle$ direction but not along the $\langle 001 \rangle$ direction.²⁰ Accordingly, intrinsic piezoelectric fields are possible in $\langle 111 \rangle$ oriented strained layer superlattices.²¹ Experimentally, piezoelectric fields of order 200 kV/cm have

been measured in InGaAs/GaAs heterostructures.²² Simplistically, considering ordered GaInP₂ to be a GaP/InP monolayer superlattice, one might expect similar piezoelectric fields.¹⁹ For fully ordered GaInP₂ lattice matched to GaAs, the alternating GaP and InP monolayers would each be strained about 4% with the GaP under tension and the InP in compression. The piezoelectric constants, e_{14} , for GaP and InP are respectively -0.1 and $+0.04$ C/m².^{20,23-25} Hence, since both the elastic strain and the piezoelectric constant are of opposite sign in the GaP and InP layers, an intrinsic piezoelectric field is expected in this simple model.

While it is overly simplistic to model the GaP and InP monolayers in ordered GaInP₂ as simply strained bulk-like GaP and InP, intrinsic order-induced electric fields are still, in general, expected. Upon ordering, the symmetry of GaInP₂ is lowered from a cubic zinc-blende structure with point group T_d to a trigonal symmetry with point group C_{3v} with the cubic $[\bar{1}11]$ direction becoming the defining threefold rotation axis. Due to the tetrahedral bonding in a zinc-blende alloy, there is no $[\bar{1}11]$ mirror plane symmetry and hence, vector quantities such as an electric field are allowed. In general, any point group symmetry which permits a pyroelectric field also permits a ferroelectric field and vice versa.²⁵ For the particular case of ordered GaInP₂ with C_{3v} symmetry, the Ga and In planes along the $[\bar{1}11]$ direction can be offset along $[\bar{1}11]$ relative to the ideal zinc-blende positions. In a simple point ion model, any such lattice relaxation can yield a net electric field.

Using a first-principles pseudopotential method, Froyen *et al.* predict that not only should such fields exist, but that the magnitude of the expected field is 1600 kV/cm for fully ordered ($\eta=1$) GaInP₂ films.¹⁹ Furthermore, as the intrinsic field should scale as η^2 , for actual samples ($\eta \approx 0.5$), an intrinsic electric field of order 400 kV/cm is expected.^{6,19} Recent photoluminescence experiments by Ernst *et al.*²⁶ de-

^{a)}Electronic mail: JOHN_PERKINS@NREL.GOV

duce an intrinsic field of 320 kV/cm in partially ordered GaInP₂ from the Stark shift of the photoluminescence. In addition, Leong *et al.*^{27,28} explain their recent scanning capacitance microscopy and scanning near-field optical microscopy measurements on bivalent partially ordered GaInP₂ in terms of an unquantified intrinsic electric field along the $\langle 111 \rangle$ direction. On the other hand, both Alonso *et al.*²⁹ and Weil *et al.*³⁰ have found transient pyroelectricity but no steady-state electric field in partially ordered GaInP₂, consistent with a screened order-induced electric field. In short, the experiments to date provide no consensus as to the existence or strength of an order-induced electric field in GaInP₂. Accordingly, our experiments aim to determine if such strong electric fields exist in actual GaInP₂ layers similar to those currently used for both fundamental studies and prototype solar cells. For internal electric fields of order 400 kV/cm, clear Franz–Keldysh Oscillations (FKOs) would be expected in a modulated reflectance measurement.³¹ For example, the internal electric fields in strained InGaAs/GaAs heterostructures²² and multiple quantum wells³² were determined from FKOs observed in photoreflectance measurements.

We report electroreflectance measurements of ordered GaInP₂ layers. For each of two structures, two samples, with differing GaInP₂ layer thickness, were measured at $T = 100$ K. For all four samples, no FKOs are observed in unbiased electroreflectance measurements. At the lowest bias voltages for which FKOs are seen, the internal electric field in the GaInP₂ layer, as calculated from the FKOs, is ~ 60 kV/cm in all four samples. Therefore, since no FKOs are seen in the absence of an external bias, we conclude that, in our samples, any net macroscopic electric field in the GaInP₂ layer is less than ~ 60 kV/cm along the (001) direction, corresponding to ~ 100 kV/cm along the ordering direction. This upper limit is substantially lower than the 400 kV/cm predicted theoretically for GaInP₂ samples with ordering parameter $\eta = 0.5$. The possible roles of both electronic screening and domain structures are considered in light of this discrepancy.

II. EXPERIMENTAL PROCEDURES

The thin film samples used in this study were grown by atmospheric-pressure OMVPE on [001] GaAs substrates misoriented 6° towards $[111]_B$ at a sample temperature of 670°C . These growth conditions yield single variant ordered GaInP₂ layers with $\eta \approx 0.5$ for sufficiently thick layers.^{4,33} Recent photoluminescence measurements with a spatial resolution of ~ 2500 Å find a narrow distribution of the order parameter, $\eta = 0.48 \pm 0.005$ ⁶ for similarly grown samples. For these OMVPE grown samples, samples thinner than ~ 1000 Å show weaker ordering than thicker samples grown under the same conditions. Presently, these OMVPE grown GaInP₂ layers grown with no intentional doping are n type with $n_e \approx 10^{15}/\text{cm}^3$.³⁴

For the electroreflectance measurements, two different structures were fabricated, a well structure and an embedded layer structure. The inset in Fig. 1 shows the well structure. In the growth sequence, the layers are: a conducting n -GaAs

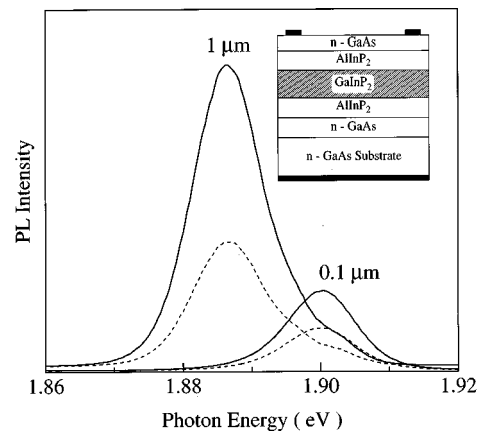


FIG. 1. Polarized photoluminescence spectra for $1 \mu\text{m}$ and $0.1 \mu\text{m}$ thick GaInP₂ well structure samples with AlInP₂ barrier layers. All spectra measured at $T = 8$ K. Solid lines for $E \parallel [1\bar{1}0]$ and dashed lines for $E \parallel [110]$ in both panels. The inset shows a typical device structure.

substrate, a 300 \AA n -GaAs buffer, a 1000 \AA AlInP₂ barrier, the ordered GaInP₂ of interest, a 1000 \AA AlInP₂ barrier and a 100 \AA n -GaAs cap. The substrate, buffer, barrier, and cap layer materials have been chosen to create nominally symmetric electronic layering around the GaInP₂ layer in order to minimize any structure induced electric fields in the GaInP₂ layer. The 100 \AA n -GaAs cap layer serves as a partially transparent conducting front contact. Electrical contacts are made via electrodeposited gold contacts on the back of the substrate and at the corners of the front surface. Two well structure samples were studied, one each with 1000 \AA and $1 \mu\text{m}$ thick GaInP₂ layers. The embedded layer structure is similar to the well structure shown in Fig. 1, but with no AlInP₂ barrier layers and p -GaAs substrate, buffer and cap layers. Embedded layer samples with 1000 and 3000 \AA GaInP₂ layers were studied. Figure 2 shows the two-point

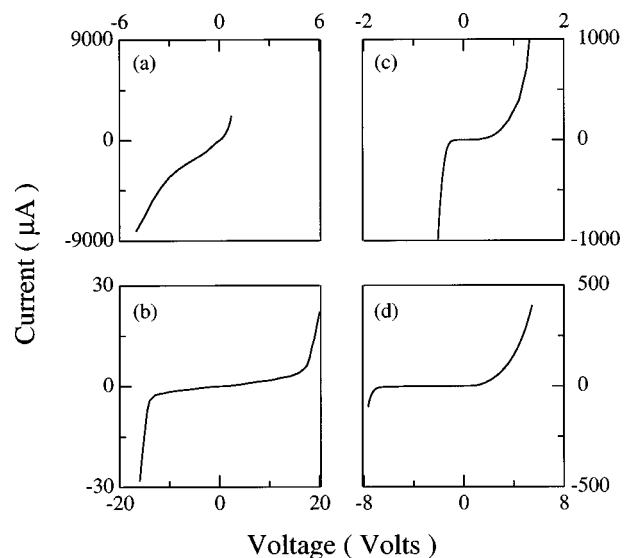


FIG. 2. I - V curves for the four GaInP₂ electromodulation devices studied. All measurements at $T = 100$ K. (A) $0.1 \mu\text{m}$ GaInP₂ well with AlInP₂ barriers and n -GaAs contacts. (B) $1 \mu\text{m}$ GaInP₂ well with AlInP₂ barriers and n -GaAs contacts. (C) $0.1 \mu\text{m}$ GaInP₂ layer with p -GaAs contacts. (D) $0.3 \mu\text{m}$ GaInP₂ layer with p -GaAs contacts.

front-back I - V curves measured at 100 K for these four samples.

The unpolarized electroreflectance spectra were measured in a near normal incidence geometry using a scanning monochromator with a broadband tungsten filament bulb as a light source. The unmodulated probe beam was focused to a roughly $1\text{ mm}\times 1\text{ mm}$ spot on the sample and the reflected light was refocused into a Si photodiode detector. A lock-in amplifier was used to measure the change in reflectance due to a modulating voltage of $\pm 0.1\text{ V}$ at 1000 Hz. Properly normalized $\Delta R/R$ spectra are obtained by simply dividing the modulated signal by the dc signal. All measurements were made at $T=100\text{ K}$ using a continuous flow cryostat. For the PL measurements, the PL was excited with a 488 nm Ar-ion laser and the spectra measured with a single grating spectrometer coupled with a LN_2 cooled CCD array. For the PL measurements, the sample was cooled to $T\approx 10\text{ K}$ with a closed-cycle cold-finger cryostat.

III. RESULTS AND DISCUSSION

Figure 1 shows polarized PL spectra measured at $T=8\text{ K}$ for two well structure samples with GaInP_2 layer thicknesses of 1000 \AA and $1\text{ }\mu\text{m}$. The PL was excited with a 488 nm Ar-ion laser running at 8 mW. An analysis polarizer at the spectrometer input is oriented parallel to either the $[1\bar{1}0]$ or the $[110]$ direction. The PL spectra for the 1000 \AA and $1\text{ }\mu\text{m}$ thick samples both show a clear polarization dependence and are peaked at lower energy than that for disordered GaInP_2 , $\sim 2.0\text{ eV}$.^{5,8} Specifically, the PL spectra are peaked at 1.901 and 1.886 eV with polarized intensity ratios of 1.91 and 2.44 for the 1000 \AA and $1\text{ }\mu\text{m}$ samples, respectively. For GaInP_2 layers ordered along the $[1\bar{1}1]$ direction, a decreased band-gap energy along with stronger PL polarized along $[1\bar{1}0]$, the projection of the $[1\bar{1}1]$ ordering direction onto the $[001]$ sample surface, is expected.^{13,18,35} Hence, the spectra in Fig. 1 show that the 1000 \AA and $1\text{ }\mu\text{m}$ well structure samples used in this study are indeed ordered. However, in the PL spectra shown in Fig. 1, only one peak per sample is evident, whereas recent PL measurements on large domain samples show two distinct peaks near the band-gap energy. The higher energy peak, absent in the PL spectra of Fig. 1, arises from the intrinsic excitonic recombination.^{33,36} The generally observed broad PL peak apparent in the PL spectra of Fig. 1 is both lower in energy than the excitonic recombination and known to blueshift with increased pump intensity.³⁷ Hence, the order parameter cannot be reliably estimated from the peak energy of the PL spectra in Fig. 1. Furthermore, since the PL polarization ratio is nearly constant for $\eta > 0.35$,¹⁸ the observed polarization ratio indicates ordering but does not provide a quantitative measure of η . Therefore, to estimate the order parameter in these samples, the $T=100\text{ K}$ band-gap energy taken from the low bias voltage electroreflectance spectra of Figs. 3, 5, 6, and 7 is used to estimate the $T=5\text{ K}$ band gap energy⁵ from which the order parameter η can be determined.^{6,8,9} The resultant order parameters range from $\eta=0.41$ to 0.47 , reasonable values for the growth parameters used. Specifically, $\eta=0.41$ and 0.46

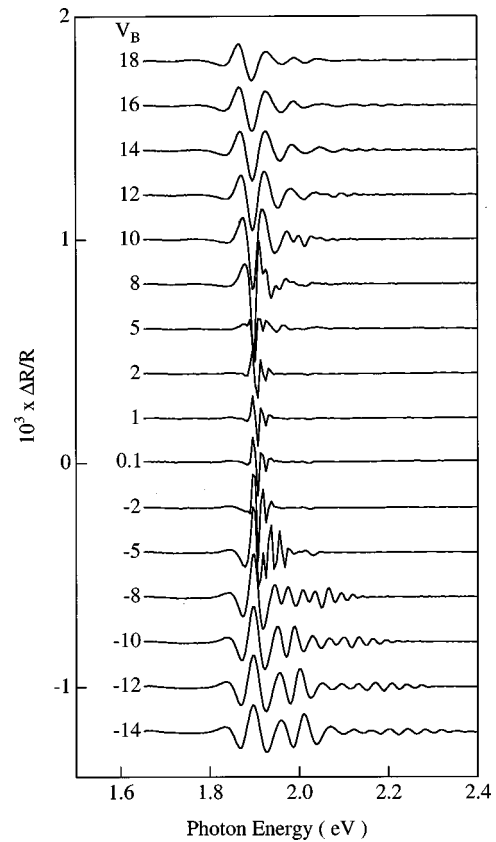


FIG. 3. Unpolarized electroreflectance spectra for $1\text{ }\mu\text{m}$ GaInP_2 well with AlInP_2 barriers measured at $T=100\text{ K}$. Spectra are labeled by applied external dc bias voltage (V_B). All spectra other than $V_B=0.1\text{ V}$ have been offset for clarity.

for the 1000 \AA and $1\text{ }\mu\text{m}$ thick well structures and $\eta=0.47$ and 0.44 for the 1000 and 3000 \AA thick embedded layer structures, respectively.

Figure 3 shows unpolarized electroreflectance spectra measured at $T=100\text{ K}$ for the well structure sample with a $1\text{ }\mu\text{m}$ GaInP_2 layer and AlInP_2 barrier layers. For each spectra the modulating voltage is the same, $\pm 0.1\text{ V}$ at 1000 Hz, but a different dc bias voltage (V_B) is applied. The useable bias voltage range, in this case -14 to $+18\text{ V}$, is determined from the I - V curve [Fig. 2(b)], also measured at $T=100\text{ K}$. All spectra other than that for $V_B=0.1$ are offset for clarity. For all the spectra, there are prominent spectral features at or near the GaInP_2 band gap, roughly 1.9 eV . However, there is a qualitative difference between the spectra measured at low bias voltages, $V_B=0.1$ – 2 V for example, and those measured at large bias voltages, $V_B=-14$ or $+18\text{ V}$. For low bias voltages, the spectral features are sharp, derivative like, localized near the band gap and, at the resolution of this measurement, show no shift in energy with changing bias voltage. In this regime, where the measured $\Delta R/R$ spectra correspond to the third derivative of the reflectance spectra with respect to the applied electric field, electroreflectance measurements are often used to determine critical point energies.^{31,38} At large bias voltages, either positive or negative, the measured spectra show broader oscillations which extend well above the band gap and do show small systematic shifts with increased bias voltage. In par-

ticular, for the $V_B = -14$ V spectra, perceptible oscillations extend up to 2.4 eV. In this high field regime, the features in the $\Delta R/R$ spectra correspond to Franz-Keldysh Oscillations and, as will be described next, the spacing between oscillation extrema are determined by the internal electric field.^{31,38}

In the presence of a uniform electric field, electronic states with a fixed energy have a spatially varying kinetic energy and hence an oscillating, but not strictly periodic, spatial wave function. When considering valence band to conduction band optical excitations, this energy dependent variation in the spatial wave function results in an oscillating energy dependent optical matrix element and hence the observed oscillating spectral features in the measured $\Delta R/R$ spectra. While an exact expression for $\Delta R/R$ can be given in terms of Airy functions,³⁸⁻⁴⁰ for strong electric fields an asymptotic approximation yields

$$\frac{\Delta R}{R} \propto \left(\frac{E_n - E_0}{\hbar \theta} \right)^{-1} \cos \left[\frac{4}{3} \left(\frac{E_n - E_0}{\hbar \theta} \right)^{3/2} + \frac{\pi}{2} \right], \quad (1)$$

where E_n is the energy of the n th extremum and $\hbar \theta$ is the electro-optical energy defined by

$$\hbar \theta = \left(\frac{e^2 \hbar^2 F^2}{2\mu} \right)^{1/3}, \quad (2)$$

where F is the internal electric field and μ is the reduced mass.^{22,38} Equation (1) makes clear the damped oscillatory nature of the FKOs. Inclusion of finite excited state lifetimes via a collisional broadening energy, Γ , yields stronger damping than in Eq. (1) but does not alter the oscillation period.^{31,38,40,41} Hence, from Eq. (1), one gets an equation relating the extremum energies in $\Delta R/R$ to the internal electric field

$$\frac{4}{3\pi} \left(\frac{E_n - E_0}{\hbar \theta_0} \right)^{3/2} = \sqrt{\frac{m_0}{\mu}} \left(\frac{F}{F_0} \right) n - \frac{1}{2} \sqrt{\frac{m_0}{\mu}} \left(\frac{F}{F_0} \right), \quad (3)$$

where n is the extremum index and $\hbar \theta_0 = 0.725 \times 10^{-3}$ eV, the electro-optical energy for $F_0 = 1$ kV/cm and $\mu = m_0$, the bare electron mass. Hence, when the extremum positions are plotted as $(E_n - E_0)^{3/2}$ vs the extremum index, a straight line is expected for FKOs with the slope proportional to the internal electric field.

Figure 4(a) shows the electroreflectance spectra for bias voltage $V_B = -12$ taken from Fig. 3 with the oscillation extrema labeled beginning from $n=0$. In Fig. 4(b), $(E_n - E_0)^{3/2}$ is plotted versus the extremum index with the same scaling used in Eq. (3). The solid line is a linear fit to the data for $n=1$ to 20. The quality of the fit supports our assertion that the observed oscillations are indeed FKOs. For $\mu/m_0 = 0.1$,^{17,42,43} the fit derived slope of 332 corresponds to an internal electric field of 105 kV/cm.

Figures 5, 6, and 7 show the electroreflectance spectra at various bias voltages for the three other samples studied, namely, a 1000 Å thick GaInP₂ well with AlInP₂ barriers, Fig. 5, and 1000 and 3000 Å thick GaInP₂ layers with p -GaAs contacts, Figs. 6 and 7, respectively. For each sample studied, the electroreflectance spectra show clear FKOs at large bias voltages and third derivative critical point spectra at low bias voltages. Since the internal electric field in the

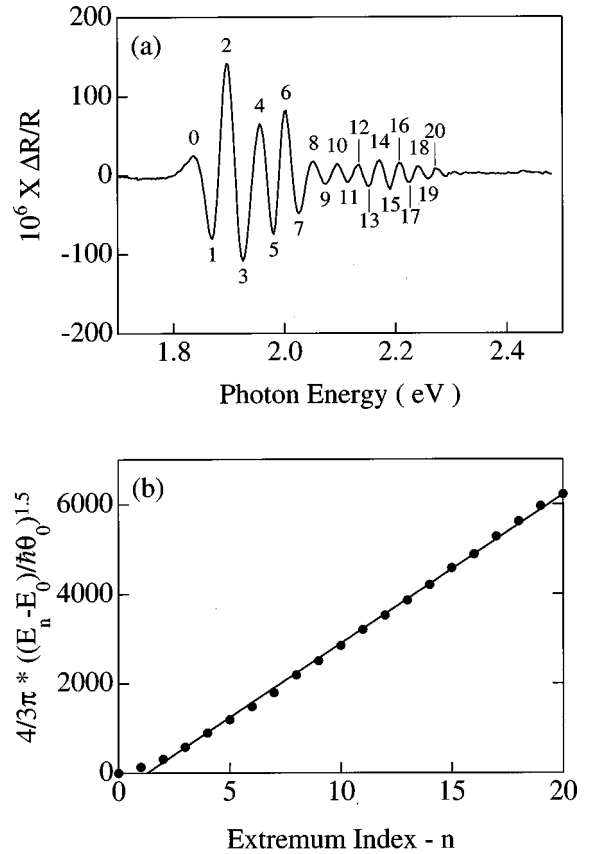


FIG. 4. Panel A: Unpolarized electroreflectance spectrum for 1 μm GaInP₂ well with AlInP₂ barriers for $V_B = -12$ V. Spectrum measured at $T = 100$ K. Clear FKOs can be seen. The oscillation extrema are indexed sequentially beginning with zero. Panel B: Oscillation extrema position plotted as $(4/3\pi)((E_n - E_0)/\hbar \theta_0)^{3/2}$ vs extremum number (n). $\hbar \theta_0 \approx 0.73 \times 10^{-3}$ eV. Solid line is a linear fit for $n=1$ to 20. Slope=332. For $\mu = 0.1m_e$, the slope of 332 corresponds to an internal electric field of 105 kV/cm in the GaInP₂ layer.

GaInP₂ layer determines whether FKO are observed, the external bias voltage at which FKOs are observed depends upon both the GaInP₂ layer thickness and the device structure. For example, the spectra in Fig. 6 for a 1000 Å thick GaInP₂ layer with no AlInP₂ barriers, FKOs are apparent at

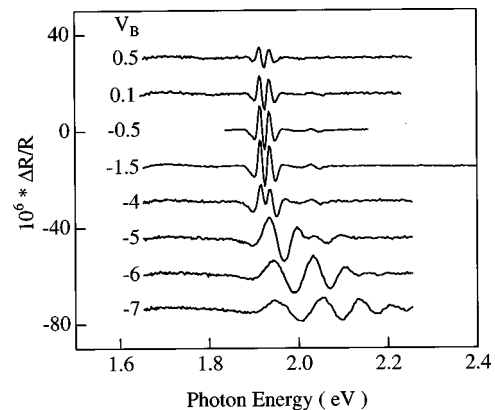


FIG. 5. Unpolarized electroreflectance spectra for 0.1 μm GaInP₂ well with AlInP₂ barriers measured at $T = 100$ K. Spectra are labeled by applied external dc bias voltage (V_B). All spectra other than $V_B = -0.5$ V have been offset for clarity.

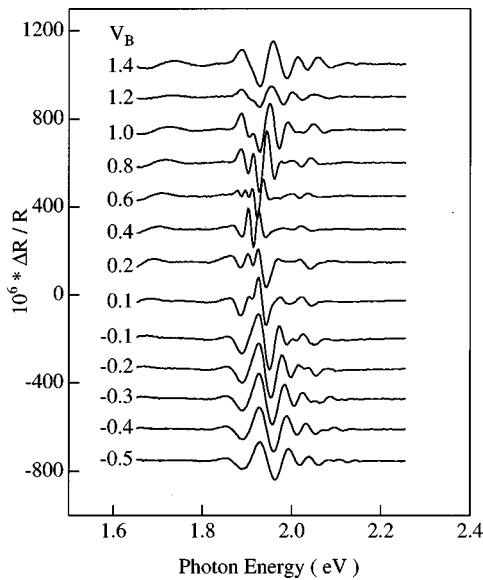


FIG. 6. Unpolarized electroreflectance spectra for $0.1 \mu\text{m}$ GaInP₂ layer with *p*-GaAs contacts measured at $T=100$ K. Spectra are labeled by applied external dc bias voltage (V_B). All spectra other than $V_B=0.1$ V have been offset for clarity.

$V_B = -0.5$ and 1.4 V. For the 1000 \AA thick GaInP₂ well with AlInP₂ barriers, a large enough positive bias voltage to induce FKO's could not be applied due to the onset of strong forward conductivity as shown by the $I-V$ curve in Fig. 2(a).

In Fig. 8, we show the FKO derived electric field strength in the GaInP₂ layer versus the nominally applied electric field for the four samples studied. The nominal electric field is simply taken to be the applied bias voltage di-

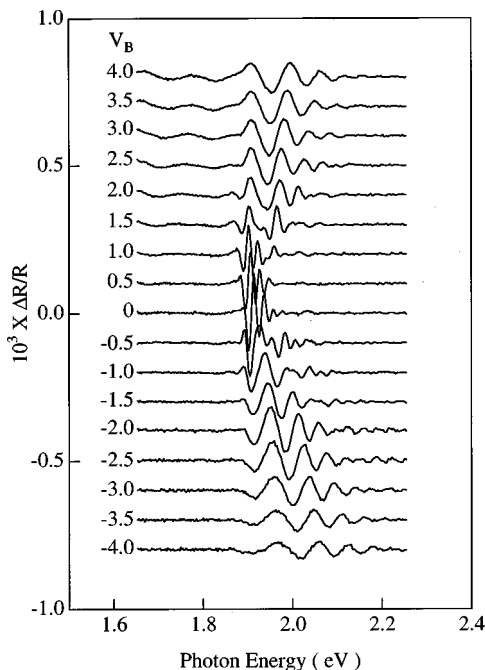


FIG. 7. Unpolarized electroreflectance spectra for $0.3 \mu\text{m}$ GaInP₂ layer with *p*-GaAs contacts measured at $T=100$ K. Spectra are labeled by applied external dc bias voltage (V_B). All spectra other than $V_B=0$ V have been offset for clarity.

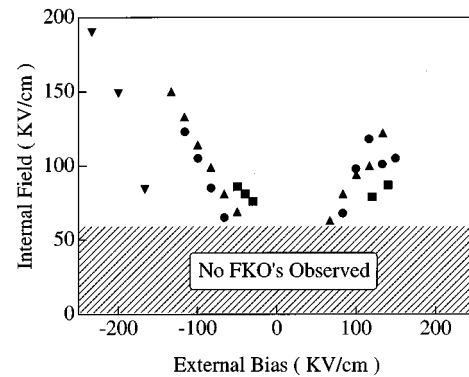


FIG. 8. Internal electric field derived from FKO vs nominal externally applied electric field for four samples. \blacktriangle : $0.3 \mu\text{m}$ GaInP₂ layer with *p*-GaAs contacts. \blacksquare : $0.1 \mu\text{m}$ GaInP₂ layer with *p*-GaAs contacts. \blacktriangledown : $0.1 \mu\text{m}$ GaInP₂ well with AlInP₂ barriers. \bullet : $1 \mu\text{m}$ GaInP₂ well with AlInP₂ barriers. The lowest internal field for which FKO are observed is about 60 kV/cm .

vided by the total thickness of the GaInP₂ layer plus the AlInP₂ barrier layers if present. All four samples show a spectroscopically derived field which increases with increasing bias voltage and is of the expected magnitude. When plotted in this manner, the relation between the spectroscopically derived electric field and the nominal externally applied electric field is approximately device independent, suggesting that these results are representative of the electric field in the GaInP₂ layer. The slight exception is the 1000 \AA well structure sample, in which, for a given externally applied field, the spectroscopically determined field in the GaInP₂ layer is noticeably less than that for the other three devices. However, for this device, the combined AlInP₂ barrier thickness included in calculating the nominal applied field is twice the GaInP₂ layer thickness. Hence, assuming a larger voltage drop across the insulating AlInP₂ barrier than in the GaInP₂, the calculated externally applied field likely substantially overestimates the actual field, consistent with the results shown in Fig. 8.

Figure 8 also makes clear two important results of this study. First, in our ordered GaInP₂ samples, the minimum internal electric field necessary for observation of clear FKO's is about 60 kV/cm and second, no FKO's are seen at zero bias voltage. A $[1\bar{1}1]$ oriented intrinsic field would have components both parallel and perpendicular to the growth direction $[001]$. For our device structure (Fig. 1 inset), carriers in the conducting front and back contacts should screen any electric field component perpendicular to $[001]$. Therefore, the 60 kV/cm limit for observation of $[001]$ fields by FKO's corresponds to roughly a 100 kV/cm limit for intrinsic order-induced fields along the ordering direction $[1\bar{1}1]$ for our OMVPE grown samples. This upper limit is substantially lower than the 400 kV/cm predicted theoretically for GaInP₂ samples with ordering parameter $\eta=0.5$.

There are several caveats regarding our findings. First, since the observed FKO's in $\Delta R/R$ invert if the applied field is reversed and our measurements average over a large sample volume, strong intrinsic fields might not yield measurable FKO's if the net field cancels out when averaged over an ensemble of domains. Reversal of the Ga/In ordering se-

quence due to a CuPt antiphase boundary⁴⁴ could yield such domains with oppositely oriented internal fields and hence no net spatially averaged field. Second, the inherent unintentional *n*-type doping level for similar OMVPE grown GaInP₂ layers is $\sim 10^{15}/\text{cm}^3$. The calculations of Froyen *et al.*,¹⁹ which predict strong internal electric fields, are for perfect, carrier-free GaInP₂. The electric field due to a sheet charge of 10^{11} electrons/cm², corresponding to all the electrons in a 1 μm layer with $n_e = 10^{15}/\text{cm}^3$, is ~ 100 kV/cm. Hence, in orders of magnitude, sufficient carrier density may exist to screen an order-induced electric field even if such a field would exist in perfect carrier-free ordered GaInP₂.

The observation of well defined excitons in photoluminescence,^{33,36} photoluminescence excitation,⁸ and exciton absorption bleaching studies⁹ further suggests that no strong internal fields are present within individual ordered domains of the measured samples. For excitons with a reduced mass $\mu \approx 0.1m_e$ in a dielectric with $\epsilon \approx 13$, the exciton binding energy and Bohr radius are roughly 10 meV and 10 nm, respectively. Hence, for electric fields greater than roughly 10 kV/cm, no excitonic bound state would exist. Experimentally, excitons in GaAs/AlGaAs heterostructures have been shown to disappear upon application of a 10 kV/cm field.⁴⁵ At first, this appears to be irreconcilable with the results of Ernst *et al.*,²⁶ who measured the electric field dependence of the PL up to total fields of order 200 kV/cm including the built in field due to their *p-i-n* device structure. However, in the work of Ernst *et al.*, the 200 Å thick ordered GaInP₂ layer embedded in disordered GaInP₂ barrier layers forms a quantum well thereby providing additional electron-hole confinement.

Transient pyroelectricity has also been observed in ordered GaInP₂,²⁹ consistent with a screened order-induced electric field. Simply put, the lattice parameters change with temperature and hence the strength of an order-induced field would change as well. However, if the sample can be heated quickly with respect to the screening time, a transient measurable pyroelectric voltage will appear even when no steady state voltage exists. Recent experiments by Weil *et al.*³⁰ both confirm the existence of pyroelectricity in ordered GaInP₂ and find a quadratic dependence on the order parameter, as would be expected for pyroelectricity due to cation ordering. Screening is common in pyroelectric materials due to either imperfect insulation or surface charges accumulated from the environment.²⁵ In the experiments on $\langle 111 \rangle$ strained layer InGaAs/GaAs and InAlAs/AlAs heterostructures, which observe steady state piezoelectric fields of order 200 kV/cm, either the measurements were done at $T = 5$ K on undoped samples⁴⁶ or on devices with a built in bias field such that the strained layer was carrier free.^{19,22,32}

Leong *et al.* suggest that their recent scanning capacitance microscopy²⁷ and scanning near-field optical microscopy²⁸ measurements on bivalent ordered GaInP₂ are supportive of intrinsic internal fields. In their experiments, Leong *et al.* find both *n*- and *p*-type regions which are spatially correlated with domain boundaries between $[111]$ and $[\bar{1}\bar{1}\bar{1}]$ ordered facets. An order-induced field in such samples would lead to oscillating band bending spatially correlated with the ordered facets and hence possibly to alternating *n*-

and *p*-type regions. While Leong *et al.* do not provide a quantitative estimate of the field required, for this model to explain the observed *n*- and *p*-type regions, the field must be of the order of the band gap divided by the domain size, ~ 2 eV per 2 μm or 10 kV/cm. Hence, while these experiments are consistent with the existence of internal fields, they do not provide much support for the existence of intrinsic fields of order 400 kV/cm. Leong *et al.* also state that dopant segregation due to the faceted surface could provide the internal electric field necessary to explain the spatially varying *n*- and *p*-type regions observed. Froyen *et al.* point out that even in perfect carrier-free ordered GaInP₂, screening by tunneling will limit any field to the band gap divided by the domain size. However, for our 1000 Å thick samples, this corresponds to roughly 200 kV/cm, a field which should be observable by our electroreflectance measurements.

IV. SUMMARY

Recent calculations by Froyen *et al.*¹⁹ suggest that an intrinsic ordering-induced electric field of order 1600 kV/cm should exist in perfectly ordered ($\eta = 1$) insulating GaInP₂ layers. Since such a field should scale as η^2 , a field of order 400 kV/cm is expected for actual samples with $\eta \approx 0.5$. For such a strong internal electric field, clear FKOs would be expected in electroreflectance measurements. We have measured the $T = 100$ K electroreflectance spectra of four ordered GaInP₂ samples with $\eta \approx 0.45$. For each of two structures, two samples with different thickness GaInP₂ layers were measured. For all four samples, no FKOs are observed in electroreflectance measurements with no external dc bias voltage applied. When a sufficiently large dc bias voltage is applied, clear FKOs are observed in all four samples. We find that the minimum internal electric field for well defined FKOs in GaInP₂, as calculated from the FKOs, is about 60 kV/cm in the $[001]$ direction, corresponding to about 100 kV/cm along the $[111]$ ordering direction. Hence, since no FKOs are observed at zero bias, we conclude that, in our OMVPE grown ordered GaInP₂ layers, any net macroscopic internal electric field is necessarily less than about 100 kV/cm along the ordering direction.

This upper limit is substantially lower than both the 400 kV/cm predicted theoretically¹⁹ for partially ordered GaInP₂ with $\eta \approx 0.5$ and the 320 kV/cm deduced from Stark effect measurements.²⁶ In our OMVPE grown samples, an order-induced electric field could either be electronically screened due to the background carrier concentration or be unobservable by FKOs due to a domain structure such that the spatially averaged field is weak. However, the experimental observation of well defined excitons in similarly grown GaInP₂ samples also suggests that no strong internal fields exist.

Collectively, these experiments suggest that no strong steady-state internal electric fields exist in our 1000 Å to 2 μm thick OMVPE grown ordered GaInP₂ layers. On the other hand, the observation of transient pyroelectricity in similar GaInP₂ samples suggests a screened order-induced field, consistent with the C_{3v} symmetry of ordered GaInP₂. Our electromodulation measurements, the observation of excitons in PL measurements and transient pyroelectricity but

not a steady-state electric field are all consistent with a screened order-induced field of unknown magnitude. Further experimental work on more insulating samples with device structures designed to yet further reduce the carrier concentration in the ordered GaInP₂ layers may enable more quantitative limits on the properties of perfect carrier-free ordered GaInP₂. Likewise, calculations aimed at understanding the effect of finite doping levels on the predicted fields would be valuable.

ACKNOWLEDGMENTS

The authors thank C. Kramer for help with sample preparation and H. Cheong, F. A. J. M. Driessen, S. Froyen, and A. Zunger for informative discussions. This work was supported by the Office of Energy Research (Materials Science Division) of the Department of Energy under Contract No. DE-AC36-83CH10093.

- ¹A. Gomyo, T. Suzuki, and S. Iijima, *Phys. Rev. Lett.* **60**, 2645 (1988).
- ²A. Mascarenhas, S. Kurtz, A. Kibbler, and J. M. Olson, *Phys. Rev. Lett.* **63**, 2108 (1989).
- ³S. R. Kurtz, J. M. Olson, and A. Kibbler, *Appl. Phys. Lett.* **57**, 1922 (1990).
- ⁴S. R. Kurtz, J. M. Olson, D. J. Arnet, M. H. Bode, and K. A. Bertness, *J. Appl. Phys.* **75**, 5110 (1994).
- ⁵R. G. Alonso, A. Mascarenhas, G. S. Horner, K. A. Bertness, S. R. Kurtz, and J. M. Olson, *Phys. Rev. B* **48**, 11 833 (1993).
- ⁶H. M. Cheong, A. Mascarenhas, J. F. Geisz, J. M. Olson, M. W. Keller, and J. R. Wendt, *Phys. Rev. B* **57**, R9400 (1998).
- ⁷G. S. Horner, A. Mascarenhas, R. G. Alonso, S. Froyen, K. A. Bertness, and J. M. Olson, *Phys. Rev. B* **49**, 1727 (1994).
- ⁸P. Ernst, C. Geng, F. Scholz, H. Schweizer, Y. Zhang, and A. Mascarenhas, *Appl. Phys. Lett.* **67**, 2347 (1995).
- ⁹B. Fluegel, Y. Zhang, H. M. Cheong, A. Mascarenhas, J. F. Geisz, J. M. Olson, and A. Duda, *Phys. Rev. B* **55**, 13 647 (1997).
- ¹⁰S.-H. Wei and A. Zunger, *Appl. Phys. Lett.* **56**, 662 (1990).
- ¹¹S.-H. Wei, D. B. Laks, and A. Zunger, *Appl. Phys. Lett.* **62**, 1937 (1993).
- ¹²S.-H. Wei and A. Zunger, *Phys. Rev. B* **49**, 14 337 (1994).
- ¹³S.-H. Wei and A. Zunger, *Appl. Phys. Lett.* **64**, 1676 (1994).
- ¹⁴A. Zunger and S. Mahajan, in *Handbook of Semiconductors*, edited by T. S. Moss (Elsevier Science B.V., Amsterdam, 1994), Vol. 3, p. 1399.
- ¹⁵Y. C. Yeo, M. F. Li, T. C. Chong, and P. Y. Yu, *Phys. Rev. B* **55**, 16 414 (1997).
- ¹⁶J. S. Luo, J. M. Olson, Y. Zhang, and A. Mascarenhas, *Phys. Rev. B* **55**, 16 385 (1997).
- ¹⁷Y. Zhang and A. Mascarenhas, *Phys. Rev. B* **51**, 13 162 (1995).
- ¹⁸Y. Zhang, A. Mascarenhas, P. Ernst, F. A. J. M. Driessen, D. J. Friedman, K. A. Bertness, and J. M. Olson, *J. Appl. Phys.* **81**, 6365 (1997).
- ¹⁹S. Froyen, A. Zunger, and A. Mascarenhas, *Appl. Phys. Lett.* **68**, 2852 (1996).
- ²⁰R. M. Martin, *Phys. Rev. B* **5**, 1607 (1972).
- ²¹D. L. Smith and C. Mailhot, *Phys. Rev. Lett.* **58**, 1264 (1987).
- ²²H. Shen, M. Dutta, W. Chang, R. Moerkirk, D. M. Kim, K. W. Chung, P. P. Ruden, M. I. Nathan, and M. A. Stroschio, *Appl. Phys. Lett.* **60**, 2400 (1992).
- ²³W. F. Boyle and R. J. Sladek, *Solid State Commun.* **16**, 323 (1975).
- ²⁴D. F. Nelson and E. H. Turner, *J. Appl. Phys.* **39**, 3337 (1968).
- ²⁵J. F. Nye, *Physical Properties of Crystals* (Oxford University Press, Oxford, 1985).
- ²⁶P. Ernst, C. Geng, M. Burkard, F. Scholz, and H. Schweizer, in *Proceedings of the 23rd International Conference on The Physics of Semiconductors*, edited by M. Scheffler and R. Zimmermann (World Scientific, Singapore, 1996), Vol. 1, p. 469.
- ²⁷J.-K. Leong, C. C. Williams, J. M. Olson, and S. Froyen, *Appl. Phys. Lett.* **69**, 4081 (1996).
- ²⁸J.-K. Leong, C. C. Williams, and J. M. Olson, *Phys. Rev. B* **56**, 1472 (1998).
- ²⁹R. G. Alonso, A. Mascarenhas, G. S. Horner, K. Sinha, J. Zhu, D. J. Friedman, K. A. Bertness, and J. M. Olson, *Solid State Commun.* **88**, 341 (1993).
- ³⁰R. Weil, A. Chack, M. Levy, J. Salzman, and R. Beserman, *J. Appl. Phys.* **81**, 3729 (1997).
- ³¹H. Shen and M. Dutta, *J. Appl. Phys.* **78**, 2151 (1995).
- ³²S. A. Dickey, A. Majerfeld, J. L. Sánchez-Rojas, A. Sacedón, E. Muñoz, A. Sanz-Hervás, M. Aguilar, and B. W. Kim, *Proceedings of the Low Dimensional Semiconductor Devices* (unpublished).
- ³³H. M. Cheong, A. Mascarenhas, S. P. Ahrenkeil, K. M. Jones, J. F. Geisz, and J. M. Olson, *J. Appl. Phys.* **83**, 5418 (1998).
- ³⁴S. R. Kurtz, J. M. Olson, D. J. Friedman, A. E. Kibbler, and S. Asher, *J. Electron. Mater.* **23**, 431 (1994).
- ³⁵A. Mascarenhas and J. M. Olson, *Phys. Rev. B* **41**, 9947 (1990).
- ³⁶P. Ernst, C. Geng, G. Hahn, F. Scholz, H. Schweizer, F. Philipp, and A. Mascarenhas, *J. Appl. Phys.* **79**, 2633 (1996).
- ³⁷P. Ernst, C. Geng, F. Scholz, and H. Schweizer, *Phys. Status Solidi B* **193**, 213 (1996).
- ³⁸D. E. Aspnes and N. Bottka, in *Semiconductors and Semimetals*, edited by R. K. Willardson and A. C. Beer (Academic, New York, 1972), Vol. 9, p. 457.
- ³⁹M. Abramowitz and I. A. Stegun, *Handbook of Mathematical Functions* (Dover, New York, 1972).
- ⁴⁰D. E. Aspnes, *Phys. Rev. B* **10**, 4228 (1974).
- ⁴¹F. H. Pollak and H. Shen, *Mater. Sci. Eng.*, **R. 10**, 275 (1993).
- ⁴²P. Ernst, Y. Zhang, F. A. J. M. Driessen, A. Mascarenhas, E. D. Jones, C. Geng, F. Scholz, and H. Schweizer, *J. Appl. Phys.* **81**, 2814 (1997).
- ⁴³Y. Zhang, A. Mascarenhas, and E. D. Jones, *J. Appl. Phys.* **83**, 448 (1998).
- ⁴⁴C. S. Baxter, W. M. Stobbs, and J. H. Wilkie, *J. Cryst. Growth* **112**, 373 (1991).
- ⁴⁵D. A. B. Miller, D. S. Chemla, T. C. Damen, A. C. Gossard, W. Wiegmann, T. H. Wood, and C. A. Burrus, *Phys. Rev. B* **32**, 1043 (1985).
- ⁴⁶P. J. Harshman and S. Wang, *J. Appl. Phys.* **71**, 5531 (1992).